Biological Conservation 258 (2021) 109128

Contents lists available at ScienceDirect

Biological Conservation

journal homepage: www.elsevier.com/locate/biocon

Incorporating climate change in a harvest risk assessment for polar bears *Ursus maritimus* in Southern Hudson Bay

Eric V. Regehr [a,*], Markus Dyck [b,1], Samuel Iverson [c], David S. Lee [d], Nicholas J. Lunn [e], Joseph M. Northrup [f,j], Marie-Claude Richer [g], Guillaume Szor [h], Michael C. Runge [i]

[a] Polar Science Center, Applied Physics Laboratory, University of Washington, Seattle, Washington 98105, USA
[b] Department of Environment, Government of Nunavut, Igloolik, Nunavut X0A 0L0, Canada
[c] Environment and Climate Change Canada, Canadian Wildlife Service, Gatineau, Québec K1A 0H3, Canada
[d] Department of Wildlife and Environment, Nunavut Tunngavik Inc., Ottawa, Ontario K1P 5E7, Canada
[e] Environment and Climate Change Canada, Biological Sciences Building, University of Alberta, Edmonton, Alberta T6G 2E9, Canada
[f] Ontario Ministry of Natural Resources and Forestry, Peterborough, Ontario K9L 1Z8, Canada
[g] Ministère des Forêts, de la Faune et des Parcs, Gouvernement du Québec, Québec City, Québec G1S 4X4, Canada
[h] Ministère des Forêts, de la Faune et des Parcs, Gouvernement du Québec, Chibougamau, Québec G8P 2Z3, Canada
[i] U.S. Geological Survey, Eastern Ecological Science Center, Patuxent Research Refuge, Laurel, Maryland 20708, USA
[j] Environmental and Life Sciences Graduate Program, Trent University, Peterborough, Ontario K9L 1Z8, Canada

ARTICLE INFO

Keywords:
Arctic
Climate warming
Habitat loss
Hunting
State-dependent management
Subsistence
Sustainability

ABSTRACT

Arctic marine mammals are harvested by Indigenous people for subsistence and are socially and culturally important. For ice-dependent species like the polar bear *Ursus maritimus*, management and conservation require understanding interactions between harvest and sea-ice loss due to climate change. We developed a demographic model to evaluate harvest risk for polar bears in Southern Hudson Bay, Canada, where the annual ice-free season has increased by approximately one month in recent decades. The model was based on the theta-logistic equation and allowed for density-dependent changes (through carrying capacity [*K*]) and density-independent changes (through population growth rate [*r*]). Model parameters were estimated using a Bayesian Monte Carlo method that included capture-recapture, aerial survey, and harvest data. Harvest management followed a state-dependent approach under which new estimates of abundance were used to update the harvest level every five years. Under a middle-of-the-road environmental scenario that assumed *K* and *r* would decline in proportion to projected sea-ice declines, annual removal of 0.02–0.03 of females resulted in a 0.8 probability of maintaining subpopulation abundance above maximum net productivity level for three polar bear generations (~34 years), our primary criterion for sustainability. Under more pessimistic and optimistic environmental scenarios, comparable female harvest rates were 0.01 and 0.055, respectively. Our coupled modeling-management framework can be used to inform tradeoffs between protection and sustainable use for wildlife populations experiencing habitat loss.

1. Introduction

Flexible and adaptive management is required to address the fast pace of ecological change in the Arctic (Post et al., 2019) and the variable, often poorly understood, effects it is having on wildlife (e.g., Descamps et al., 2017). For harvested species, scientific assessment of interactions between harvest and climate change can help resource managers balance the demographic effects of human-caused removals with the nutritional, social, and economic benefits of use (Bowyer et al., 2019). As environmental conditions move farther from historical baselines (IPCC, 2019), conservation of Arctic fauna will depend on the ability to articulate clear management objectives, evaluate population status using models that account for climate change, and implement effective co-management between local users and resource managers (Laidre et al., 2015).

Polar bears (*Ursus maritimus*) depend on sea ice for critical aspects of

* Corresponding author.
E-mail address: eregehr@uw.edu (E.V. Regehr).
[1] Deceased 25 April 2021.

https://doi.org/10.1016/j.biocon.2021.109128
Received 12 June 2020; Received in revised form 7 April 2021; Accepted 9 April 2021
Available online 19 May 2021

their life history, including access to their primary prey, ringed seals *Pusa hispida*) and bearded seals (*Erignathus barbatus*; Amstrup, 2003). The Arctic is warming faster than other parts of the planet (Post et al., 2019) and the resulting sea-ice loss is considered the primary threat to the species (PBRS, 2015). Although most polar bears are expected to be negatively affected by climate change in the long term (Atwood et al., 2016), the 19 recognized subpopulations currently exhibit variable status due to differences in physical geography, biological productivity, and other factors (Durner et al., 2018). Most polar bear subpopulations are subject to a legal and managed subsistence harvest by Indigenous people (Laidre et al., 2015). Thus, a primary goal of polar bear management is to estimate the number of bears that can be removed annually while meeting population management objectives. Harvest risk assessment methods that allow for climate-driven changes in demographic parameters have been developed recently (Regehr et al. 2017) but require detailed vital rate estimates that are only available for some polar bear subpopulations (e.g., Regehr et al., In press).

The Southern Hudson Bay (SH) polar bear subpopulation occurs near the southern limit of the species' range (Fig. 1) where the ice melts completely each summer. Since 1979, marine waters within the SH subpopulation boundary have lost approximately seven ice-covered days per decade (a metric used to quantify the time available for polar bears to hunt seals; Stern and Laidre, 2016). Intermittent live-capture studies suggest that SH polar bear body condition (i.e., fatness) declined over the period 1984–2009, likely in response to habitat loss (Obbard et al., 2016). The most recent estimate of total (i.e., female and male) subpopulation abundance was 780 bears (95% confidence interval [CI] = 590–1029) in 2016 (Obbard et al., 2018), which represents a likely decline from the previous estimate of 943 bears (95% CI = 658–1350) in 2012 (Obbard et al., 2015). In the adjacent Western Hudson Bay (WH) subpopulation, where live-capture research occurs annually, declines in body condition were detected prior to declines in reproduction, survival, and abundance (Lunn et al., 2016). As an expression of Indigenous Knowledge (IK), individuals and communities in the SH region recognize environmental changes but consider polar bear abundance as stable or increasing, and express concern about increasing human-polar bear interactions and threats to human safety (Tonge and Pulfer, 2011; Laforest et al., 2018; NMRWB, 2018). Polar bears from the SH subpopulation are actively harvested by Indigenous communities.

We developed a demographic model for the female component of the SH polar bear subpopulation based on a discrete version of the theta-logistic equation, which has been widely used to evaluate wildlife harvest (e.g., Johnson et al., 2018). Our goal was to forecast the demographic effects of different harvest strategies over the next 34 years (approximately three polar bear generations; Regehr et al., 2016). In this paper, "harvest" refers to all human-caused removals (i.e., the combination of subsistence harvest, removal of bears in defense of life and property, and other direct human-caused mortality). The potential effects of climate warming were represented via changes in habitat quantity affecting the number of animals the environment can support (through the theta-logistic parameter for environmental carrying capacity [K]), and changes in habitat quality affecting population growth regardless of density (through the theta-logistic parameter for intrinsic growth rate [r_{max}]; USFWS, 2016). We accounted for sampling uncertainty by using population reconstruction (e.g., Nilsen and Strand, 2018) to estimate parameters of the theta-logistic equation from historical capture-recapture, aerial survey, and harvest data. We accounted for environmental uncertainty by developing alternative scenarios informed by scientific studies, IK, and projections of sea ice. Analyses followed a state-dependent approach under which harvest levels were updated periodically using new data on the demographic status (i.e.,

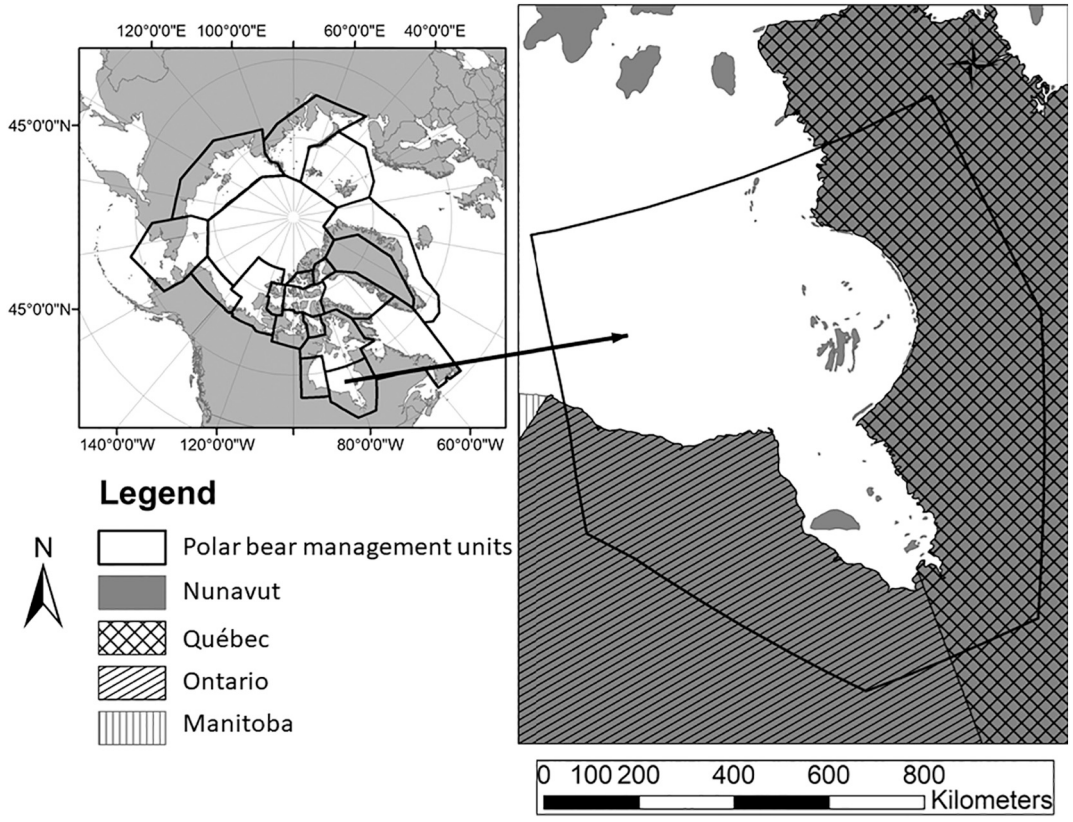

Fig. 1. Area of the Southern Hudson Bay (SH) polar bear subpopulation (right), which is among the southernmost of the world's 19 recognized polar bear subpopulations (left). Subpopulation boundaries generally correspond to management units for the species. SH bears are harvested for subsistence by hunters from Nunavut, Ontario, and Québec.

"state") of the subpopulation (Runge et al., 2009).

2. Materials and methods

2.1. Data for the SH polar bear subpopulation

Empirical data for the SH subpopulation included harvest records, estimates of abundance from capture-recapture studies and aerial surveys, and estimates of population growth rate calculated using vital rates from capture-recapture studies. We modeled the female component of the SH subpopulation only because females are the most important contributors to population growth (Hunter et al., 2007) and aerial surveys in the 2010s did not provide detailed information on subpopulation composition. The data are described below and their use to estimate parameters of the theta-logistic equation is described in the section Bayesian population reconstruction.

Female harvest data were obtained from management authorities responsible for the SH polar bear subpopulation (Nunavut, Ontario, and Québec). To account for incomplete reporting, we treated annual harvest as a random variable based on reported harvest levels and estimates of reporting probability (Supporting File 1).

Estimates of total (i.e., female and male) abundance (N^{f+m}) were available for the periods 1984–1986 and 2003–2005 from capture-recapture studies (Kolenosky et al., 1992; Obbard et al., 2007) and for the years 2012 and 2016 from distance-sampling aerial surveys (Obbard et al., 2015, 2018). The capture-recapture estimates were adjusted upwards to account for incomplete geographic sampling and improve consistency with the aerial survey estimates (Supporting File 2). The resulting numbers for N^{f+m}, and the proportion of females in the subpopulation ($prop_{af}$), were 802 bears (95% confidence interval [CI] = 564–1044, $prop_{af} = 0.46$) in 1986, 842 (95% CI = 564–1118, $prop_{af} = 0.57$) in 2005, 943 (95% CI = 650–1312, $prop_{af} = 0.50$) in 2012, and 781 (95% CI = 590–1023, $prop_{af} = 0.50$) in 2016. These data were used to calculate female abundance (N).

We calculated values of female population growth rate (r) referenced to 1986 and 2005 using survival rates from Obbard et al. (2007, 2010) and reproductive parameters from Kolenosky et al. (1994) and Obbard et al. (2010). First, we used a stage-structured matrix population model for polar bears (Hunter et al., 2010) to calculate asymptotic, observed growth rate (r_{obs}) based on the published estimates of total female survival (S^{total}), which included harvest mortality. Second, we converted estimates of S^{total} to unharvested survival (S) using the formula:

$$S = S^{total}/(1 - H/N), \tag{1}$$

where H is the number of females removed by humans. Thus, H/N is the female harvest mortality rate (h). We then used estimates of S (Supporting File 2) in the matrix model to calculate potential growth rates in the absence of harvest. We denote these growth rates r_{MNPL} because they were referenced to a subpopulation density at maximum net productivity level (*MNPL*), the subpopulation size that results in the greatest net annual increment in numbers resulting from reproduction minus losses due to natural mortality. By referring to these growth rates as r_{MNPL}, we assume that the SH subpopulation has been harvested in the vicinity of maximum sustainable yield (*MSY*) in recent decades (Obbard et al., 2007). Finally, we estimated maximum intrinsic growth rate (r_{max}) using the ratio $r_{MNPL}/r_{max} = 0.82$ that has been suggested for polar bears (Regehr et al. 2017). We accounted for statistical uncertainty in estimates of r by generating 10,000 random samples of the vital rates (i.e., breeding and survival probabilities) using the published means and variances and a correlation matrix from the most supported capture-recapture model in Obbard et al. (2007).

2.2. Demographic model

The theta-logistic equation can be written as follows:

$$N_{t+1} = N_t(1-h) \times exp\left\{ r_{max}\left[1 - \left(\frac{N_t(1-h)}{K_t}\right)^{\theta}\right]\right\} \tag{2}$$

where N is abundance, r_{max} is maximum intrinsic growth rate, K is environmental carrying capacity, h is the harvest rate (i.e., the proportion of subpopulation abundance removed annually), and θ is a shape parameter that determines how the growth rate changes as a function of density. Parameters are referenced to females unless otherwise noted. The annual harvest level (i.e., the number of bears removed from the subpopulation between time steps t and $t + 1$) is calculated as $H_t = hN_t$. For most analyses, we fixed θ to 5.045 because this value produces dynamics that are typical of long-lived mammals (Wade, 1998) and consistent with other models for polar bears (Appendix 1; USFWS, 2016). Our simulations considered changes in both K and r_{max} but did not include a mechanistic link between the two parameters. We quantified habitat loss and its potential effects on demography by using the number of ice-covered days per year within the SH subpopulation boundary, derived from remote-sensing data using the methods of Stern and Laidre (2016) and projected forward (Supporting File 3), as a proxy for trends and variation K.

2.3. State-dependent harvest management framework

We modeled a state-dependent harvest management framework under which new demographic data were used to periodically update the harvest level. For a given harvest strategy, H_t was calculated as the product of h and $\widetilde{N}_t$, a median estimate of female abundance available at time step t. During population projections (see section Simulations to evaluate harvest risk), values of $\widetilde{N}_t$ were obtained from simulated research studies according to the management interval (i.e., the number of years elapsed between updates to harvest). Specifically, we randomly selected a value of N from a normal distribution with a mean equal to the mean abundance in the preceding three years and a standard deviation corresponding to $CV(\widetilde{N}) = 0.16$, the average coefficient of variation (CV) from recent aerial surveys (Obbard et al., 2015, 2018). This approach assumed that future study methods will produce estimates of mean abundance with similar precision to previous estimates and that there is a one-year lag between an estimate becoming available and its use for management.

During population projections, we recorded the probability of achieving three management objectives. Management Objective 1 sought to maintain the size of a harvested subpopulation above *MNPL*, which occurs at a relative density of approximately $N/K = 0.70$ when using $\theta = 5.045$ (Appendix 1). This objective protects against overexploitation while allowing the possibility for harvest levels to approach *MSY* (USFWS, 2016). In stochastic projections, the probability of meeting this objective at time step t was denoted $P_t^{N>MNPL}$. Management Objective 2 sought to maintain the size of a harvested subpopulation above 90% of starting abundance, similar to previous harvest risk assessments for polar bears when habitat was stable and the goal was to prevent subpopulation declines (e.g., Taylor et al., 2006a). The probability of meeting this objective at time step t was denoted $P_t^{N>0.9N1}$. Management Objective 3 conveyed whether the SH subpopulation was likely to experience severe declines. Specifically, we calculated the probability that abundance remained above a threshold value of 175 female bears at time step t ($P_t^{N>thresh}$), based on the premise that subpopulations starting at a large size (e.g., 1000) could face a heightened risk of extirpation below a total (i.e., female and male) abundance of approximately 350 (USFWS, 2016). The value 175 is a placeholder because it is not known when SH bears might experience negative small-population effects.

2.4. Bayesian population reconstruction

We used a Bayesian Monte Carlo method to estimate parameters of the theta-logistic model that provided the best fit to empirical data for the SH subpopulation. This ensured that the model could reproduce historical subpopulation trends, and provided parameter estimates for forward projections. First, we specified prior distributions for r_{max} and starting N/K (i.e., subpopulation density relative to carrying capacity at the first time step of population reconstruction) based on existing knowledge of polar bear demography and assumptions specific to each environmental scenario (see section Simulations to evaluate harvest risk and Supporting File 4). Second, we ran retrospective projections over the period 1986–2016 or a subset of these years, depending on the environmental scenario, using the theta-logistic model parameterized with 10,000 random samples from the prior distributions for r_{max} and starting N/K. Abundance at the first time step was randomly selected from a uniform distribution spanning the 95% CI of the empirical estimate of abundance for the starting year. A stochastic harvest was applied each year based on historical harvest levels (Supporting File 1), and K varied stochastically with a trend and variance specific to each scenario. Third, for each retrospective projection we calculated a likelihood based on the probabilities of observing the values of r_{max} selected from their prior distributions and the projected values of N, conditional on empirical sampling distributions of r_{max} for 1986 and 2005 from capture-recapture studies and empirical estimates of N for 1986, 2005, 2012, and 2016 from capture-recapture studies and aerial surveys (see section Data for the SH polar bear subpopulation). The log-likelihood can be written as:

$$l(\boldsymbol{\Theta}|\boldsymbol{x}) = \sum_{i=1}^{n} logP(X = x_i), \quad (3)$$

where $\boldsymbol{\Theta}$ is a vector of theta-logistic equation parameters, $\boldsymbol{x}$ is a vector of $i = 1,2, \ldots n$ observed values of r_{max} and N from a stochastic projection, x_i is the i^{th} element of $\boldsymbol{x}$, X is the empirical sampling distribution corresponding to x_i, and $P(X = x_i)$ is the probability of observing x_i given the parameter's empirical sampling distribution from research studies. Retrospective projections for which a random sample of r_{max} or a projected value of N had zero probability were discarded. For the remaining sets of theta-logistic equation parameters, we used the normalized likelihood values as observation weights to generate empirical probability density functions and posterior distributions for r_{max} and starting N/K.

2.5. Simulations to evaluate harvest risk

We used the theta-logistic model (Eq. (2)), parameterized with results of the population reconstruction, to project simulated polar bear subpopulations forward 34 years, starting in 2016 (Fig. 2). For a given projection it was necessary to specify demographic parameters of the subpopulation, environmental conditions and how they influenced

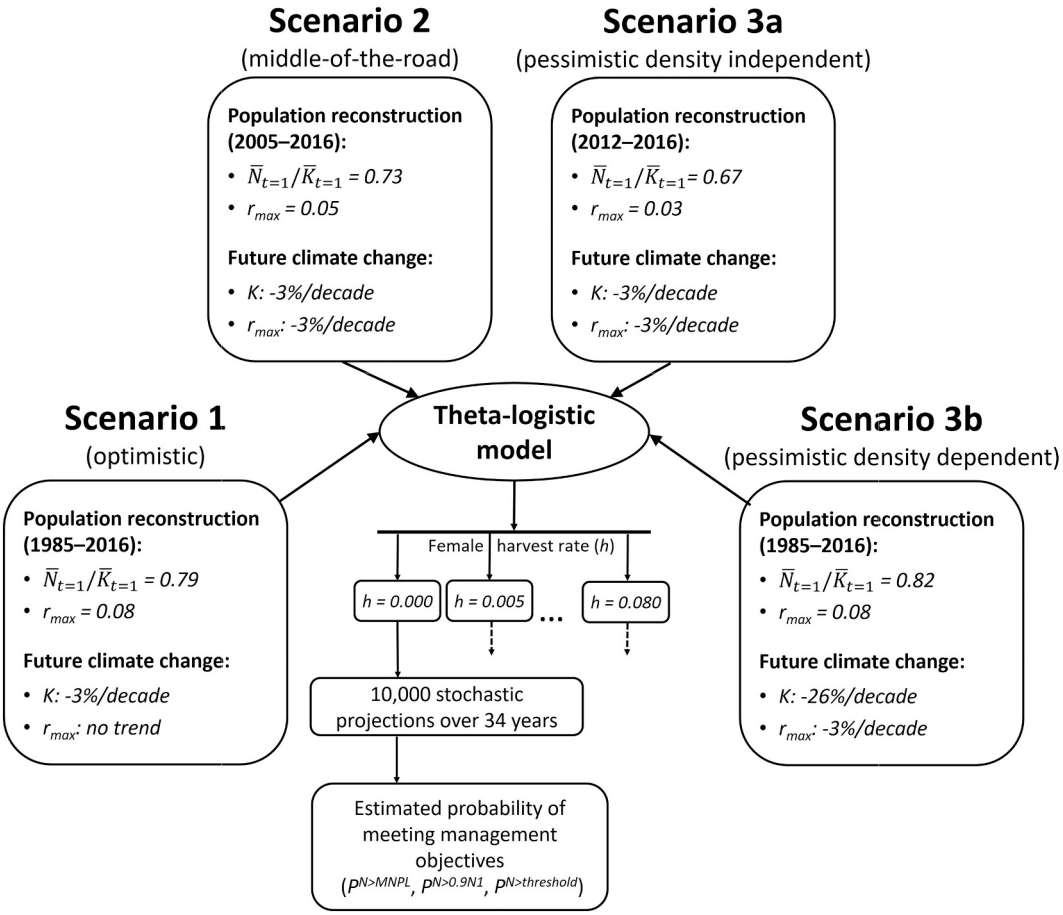

Fig. 2. Structure of the harvest risk assessment for the Southern Hudson Bay (SH) polar bear subpopulation. Scenarios represented different assumptions, from optimistic to pessimistic, about subpopulation status and the effects of climate change. Population reconstruction with demographic and harvest data for the specified period (e.g., 1985–2016) provided estimates of maximum intrinsic growth rate (r_{max}) and mean relative density at the start of forward projections ($\overline{N}_{t=1}/\overline{K}_{t=1}$, where N is abundance and K is carrying capacity). Using these estimates, subpopulations were projected forward 34 years subject to changing K and r_{max}, and female harvest at rate h. Stochastic results are presented as demographic outcomes (e.g., mean N at the end of projections; Table 1) and probabilities of meeting the three management objectives defined in the main text ($P^{N>MNPL}$, $P^{N>0.9N1}$, $P^{N>thresh}$).

demographic parameters, and a harvest strategy. Demographic parameters were $N_{t=1}$, r_{max}, and density at the first time step of forward projections (i.e., $N_{t=1}/K_{t=1}$, which together with $N_{t=1}$ permits calculation of $K_{t=1}$). Environmental conditions included temporal changes in K, r_{max}, or both. Harvest strategies were defined by a time-constant, user-specified value of h and a 5-year management interval, because the research schedule for the SH subpopulation includes aerial surveys every five years (Dyck et al., 2019). The harvest level during the first management interval (i.e., for years $t = 1, 2\ldots 5$) was calculated based on the point estimate of female abundance in 2016 (Obbard et al., 2018) for consistency across projections. At the beginning of subsequent management intervals, the harvest level was calculated using a value of $\widetilde{N}$ derived from a simulated research study.

To reflect key sources of uncertainty, we performed stochastic projections over which certain parameters varied. We defined a "simulation" as 10,000 projections with the same demographic parameters, same method to project K and specify temporal variation in r_{max}, and same harvest strategy. For each simulation, sampling variation was incorporated by selecting 10,000 random samples of r_{max} from its posterior distribution from population reconstruction, and by periodically updating the harvest level using stochastic values of $\widetilde{N}_t$. Forward projections started at a mean relative density ($\overline{N}_{t=1}/\overline{K}_{t=1}$) obtained from the final time step of population reconstruction. Environmental stochasticity between time steps t and $t + 1$ was incorporated by using a different projection of K for each sample. We recorded the probabilities of meeting the three management objectives described above, as well as mean female abundance ($\overline{N}_t$), mean environmental carrying capacity ($\overline{K}_t$), mean harvest level ($\overline{H}_t$), and the probability of extirpation, P_{ext}, defined as N falling below a quasi-extinction threshold of $0.15N_{t=1}$.

It is not possible to accurately forecast the status of the SH subpopulation under climate change based on existing information. Therefore, we performed forward projections to evaluate harvest risk under three plausible scenarios, from optimistic to pessimistic. The scenarios used theta-logistic parameters derived from population reconstruction applied to different subsets of historical data, and made different assumptions about the future effects of climate change (Fig. 2; Supporting File 4). For each scenario, we performed 17 simulations corresponding to female harvest rates from $h = 0$ to 0.08, in 0.005 increments. Scenario 1 (optimistic) assumed that the future status of the SH subpopulation will be like its average status 1986–2016, during which the subpopulation was capable of strong growth and abundance was largely stable (Supporting File 4). During forward projections, K was projected using the estimated variance and slope from a linear model fit to the sea-ice data 1979–2016, resulting in a decline of approximately 3% per decade. Scenario 2 (middle-of-the-road) assumed that the future status of the SH subpopulation will be like its average status from 2005 to 2016, during which the subpopulation was capable of moderate growth and may have experienced a decline in abundance toward the end. During forward projections, both K and r_{max} declined at 3% per decade. Scenarios 3a and 3b (pessimistic) assumed that the future status of the SH subpopulation will resemble its status 2012–2016, during which abundance likely declined. Scenario 3a attributed the decline to density-independent limitation (i.e., reduced r_{max}) whereas Scenario 3b attributed the decline to density-dependent reductions in the observed growth rate (r_{obs}) resulting from a rapidly falling K (Appendix 1). The sensitivity of projections to different values of the density-dependent parameter θ is described in Supporting File 5.

Computations were performed in the R computing language (version R 3.4.0; The R Project for Statistical Computing; http://www.r-project.org). Asymptotic growth rates were calculated from matrix projection models using the function *pop.projection* in the 'popbio' package (Stubben and Milligan, 2007).

3. Results

3.1. Data for the SH polar bear subpopulation

For the period 1985–2016, the mean female harvest level for the SH polar bear subpopulation was 19.3 bears/year (standard deviation [sd] of annual mean values = 7.9 bears/year). The mean female harvest rate, expressed as the proportion of females removed each year, was approximately 0.05 (95% CI = 0.01–0.11). Estimated growth rates in 1986 were $r_{obs} = 0.02$ (−0.07–0.08) and $r_{max} = 0.10$ (0.01–0.15), and in 2005 were $r_{obs} = -0.02$ (−0.18–0.07) and $r_{max} = 0.01$ (−0.17–0.13). The number of ice-covered days within the SH subpopulation boundary declined significantly during the period of the satellite record (1979–2016: linear model slope = −0.63 ice-covered days/year; se [slope] = 0.21, $P < 0.01$) and during the period of current modeling (1984–2016: linear model slope = −0.76 ice-covered days/year; se [slope] = 0.29, $P = 0.01$).

3.2. Simulations to evaluate harvest risk

We summarize results of the harvest risk assessment by focusing on harvest strategies with an 80% probability of meeting Management Objective 1 (i.e., $P_{t=35}^{N>MNPL} \approx 0.80$). Findings for other management objectives and risk tolerances are provided in Table 1. Results are presented up to a maximum value of $h = 0.060$, at which the probability of crossing below the minimum abundance threshold increased rapidly. Sensitivity analyses indicated that $P_{t=35}^{N>MNPL}$ was robust to changes in the density-dependent parameter θ when harvest was applied at a constant rate. Specifically, under conditions like Scenario 2 and using a female harvest rate of 0.025, values of θ = [1.0, 2.5, 5.045, 10, 15] corresponded to $P_{t=35}^{N>MNPL}$ = [0.80, 0.83, 0.84, 0.79, 0.74], respectively. Lower values of θ were associated with lower values of *MNPL* and r_{MNPL}, and therefore lower equilibrium subpopulation sizes and harvest levels (Supporting File 5).

3.3. Scenario 1

Population reconstruction provided a reasonable fit to historical data (i.e., during retrospective projections, 99% of projected values of N and r were within the 95% CIs of empirical data; Fig. 3). The posterior distribution of r_{max} had a mean of 0.08 (95% CI = 0.05–0.11; Fig. 4) and the posterior distribution of N/K at the start of population reconstruction (i.e., the value of N/K that provided the best fit to historical data) had a mean of 0.73 (95% CI = 0.53–0.89). Forward projections to evaluate harvest risk started with a relative density of $\overline{N}_{t=1}/\overline{K}_{t=1} = 0.79$, the mean value from the final time step of population reconstruction. A subpopulation with the characteristics of Scenario 1 could support a relatively high harvest (Table 1). For example, a harvest strategy with female harvest rate $h = 0.055$ resulted in $P_{t=35}^{N>MNPL} = 0.78$, which is close to an 80% probability of meeting Management Objective 1 (Fig. 5). This strategy would correspond to a starting harvest level $\overline{H}_{t=1} = 21$ female bears/year and a mean ending harvest level $\overline{H}_{t=35} = 19$ female bears/year, where the decline is due to gradual declines in projected K. Under this harvest strategy, the subpopulation would have a low probability of crossing below the minimum abundance threshold (i.e., $P_{t=35}^{N>thresh} = 0.99$) and a negligible probability of extirpation after 34 years (i.e., $P_{ext} = 0.00$). Although starting abundance was the same for all scenarios, and K declined at the same rate during forward projections for scenarios 1, 2, and 3a, $\overline{K}_{t=35}$ differed among scenarios because each started with a different value of $\overline{N}_{t=1}/\overline{K}_{t=1}$ and therefore a different value of $\overline{K}_{t=1}$.

3.4. Scenario 2

The posterior distribution of r_{max} had a mean of 0.05 (95% CI = 0.02–0.09) and the posterior distribution of N/K at the start of

Table 1
Forecasted demographic outcomes for the Southern Hudson Bay polar bear subpopulation under harvest and alternative scenarios for the current and future effects of habit loss due to climate change. h is the time-constant female harvest rate expressed as the proportion of female bears removed annually; $\overline{H}_t$ is the harvest level (female bears/year) at time step t; h^{total*} is the time-constant total (i.e., female and male) harvest rate expressed as the proportion of total bears removed annually assuming a 2:1 male-to-female ratio in removals; $\overline{N}_{t=35}$ is mean female abundance; $\overline{K}_{t=35}$ is mean environmental carrying capacity; and P_{ext} is the probability of extirpation. $P_{t=35}^{N>MNPL}$, $P_{t=35}^{N>0.9N1}$, and $P_{t=35}^{N>thresh}$ are the probabilities of meeting management objectives 1, 2, and 3, respectively. Scenarios and management objectives are defined in the main text. Most outcomes are referenced to the final time step $t = 35$.

	h	$\overline{H}_{t=1}$	h^{total*}	$\overline{N}_{t=35}$	$\overline{K}_{t=35}$	$\overline{H}_{t=35}$	$P_{t=35}^{N>MNPL}$	$P_{t=35}^{N>0.9N1}$	$P_{t=35}^{N>thresh}$	P_{ext}
Scenario 1 (optimistic)	0.000	0	0.000	424	437	0	0.99	0.97	1.00	0.00
	0.005	2	0.008	421	437	2	0.99	0.97	1.00	0.00
	0.010	4	0.015	418	437	4	0.99	0.97	1.00	0.00
	0.015	6	0.023	414	437	6	0.99	0.97	1.00	0.00
	0.020	8	0.030	410	437	8	0.99	0.97	1.00	0.00
	0.025	10	0.038	404	437	10	0.99	0.97	1.00	0.00
	0.030	12	0.045	398	437	12	0.99	0.95	1.00	0.00
	0.035	14	0.053	391	437	14	0.98	0.92	1.00	0.00
	0.040	16	0.060	382	437	16	0.97	0.85	1.00	0.00
	0.045	18	0.068	372	437	17	0.94	0.76	1.00	0.00
	0.050	20	0.075	359	437	18	0.87	0.63	1.00	0.00
	0.055	21	0.083	343	437	19	0.78	0.50	0.99	0.00
	0.060	23	0.090	324	437	20	0.67	0.36	0.97	0.00
Scenario 2 (middle-of-the-road)	0.000	0	0.000	466	474	0	1.00	1.00	1.00	0.00
	0.005	2	0.008	456	474	2	0.99	0.99	1.00	0.00
	0.010	4	0.015	443	474	4	0.99	0.98	1.00	0.00
	0.015	6	0.023	429	474	7	0.97	0.96	1.00	0.00
	0.020	8	0.030	412	474	8	0.92	0.89	1.00	0.00
	0.025	10	0.038	392	474	10	0.84	0.81	0.99	0.00
	0.030	12	0.045	369	474	11	0.75	0.70	0.98	0.00
	0.035	14	0.053	344	474	12	0.63	0.57	0.96	0.00
	0.040	16	0.060	316	474	13	0.51	0.43	0.90	0.00
	0.045	18	0.068	286	474	13	0.38	0.29	0.83	0.00
	0.050	20	0.075	255	474	13	0.26	0.19	0.74	0.00
	0.055	21	0.083	222	474	13	0.17	0.11	0.64	0.02
	0.060	23	0.090	190	474	12	0.10	0.06	0.52	0.06
Scenario 3a (pessimistic density independent)	0.000	0	0.000	492	518	0	0.99	1.00	1.00	0.00
	0.005	2	0.008	463	518	2	0.91	0.95	1.00	0.00
	0.010	4	0.015	432	518	4	0.79	0.81	1.00	0.00
	0.015	6	0.023	400	518	6	0.67	0.70	1.00	0.00
	0.020	8	0.030	367	518	8	0.56	0.59	0.98	0.00
	0.025	10	0.038	332	518	9	0.46	0.48	0.90	0.00
	0.030	12	0.045	297	518	9	0.36	0.39	0.80	0.00
	0.035	14	0.053	262	518	10	0.25	0.29	0.69	0.00
	0.040	16	0.060	227	518	10	0.15	0.18	0.58	0.00
	0.045	18	0.068	192	518	9	0.07	0.08	0.48	0.01
	0.050	20	0.075	156	518	8	0.02	0.02	0.38	0.10
	0.055	21	0.083	122	518	7	0.01	0.00	0.28	0.23
	0.060	23	0.090	92	518	6	0.00	0.00	0.19	0.35
Scenario 3b (pessimistic density dependent)	0.000	0	0.000	206	154	0	0.87	0.19	0.50	0.12
	0.005	2	0.008	199	154	1	0.85	0.19	0.48	0.15
	0.010	4	0.015	192	154	2	0.82	0.18	0.46	0.17
	0.015	6	0.023	187	154	3	0.79	0.18	0.45	0.20
	0.020	8	0.030	181	154	4	0.77	0.17	0.44	0.22
	0.025	10	0.038	176	154	5	0.75	0.16	0.43	0.24
	0.030	12	0.045	172	154	6	0.73	0.16	0.42	0.26
	0.035	14	0.053	167	154	7	0.71	0.16	0.41	0.27
	0.040	16	0.060	162	154	8	0.69	0.15	0.40	0.29
	0.045	18	0.068	158	154	9	0.68	0.14	0.40	0.30
	0.050	20	0.075	152	154	9	0.66	0.13	0.39	0.31
	0.055	21	0.083	146	154	10	0.63	0.11	0.38	0.33
	0.060	23	0.090	140	154	10	0.60	0.09	0.36	0.34

population reconstruction had a mean of 0.73 (95% CI = 0.51–0.90). Forward projections started with $\overline{N}_{t=1}/\overline{K}_{t=1} = 0.73$. A subpopulation with these characteristics could support a moderate harvest (Table 1). For example, a harvest strategy with a female harvest rate $h = 0.025$ resulted in $P_{t=35}^{N>MNPL} = 0.84$ (Fig. 5). This strategy would correspond to a starting harvest level $\overline{H}_{t=1} = 10$ female bears/year and a mean ending harvest level $\overline{H}_{t=35} = 10$ female bears/year. Under this strategy, the subpopulation would have a low probability of crossing below the minimum threshold (i.e., $P_{t=35}^{N>thresh} = 0.99$) and a negligible probability of extirpation (i.e., $P_{ext} = 0.00$).

3.5. Scenario 3

For Scenario 3a, the posterior distribution of r_{max} had a mean of 0.03 (95% CI = 0.00–0.06), like its prior. Similarly, the posterior of N/K at the start of population reconstruction had a mean of 0.71 (95% CI = 0.51–0.90). Forward projections started with $\overline{N}_{t=1}/\overline{K}_{t=1} = 0.67$. A subpopulation with these characteristics could support a low harvest (Table 1). For example, a harvest strategy with $h = 0.01$ resulted in $P_{t=35}^{N>MNPL} = 0.79$ (Fig. 5). This corresponds to a starting harvest level $\overline{H}_{t=1} = 4$ female bears/year and a mean ending harvest level $\overline{H}_{t=35} = 4$ female bears/year. Under this harvest strategy, the subpopulation would have a negligible probability of crossing below the minimum threshold (i.e.,

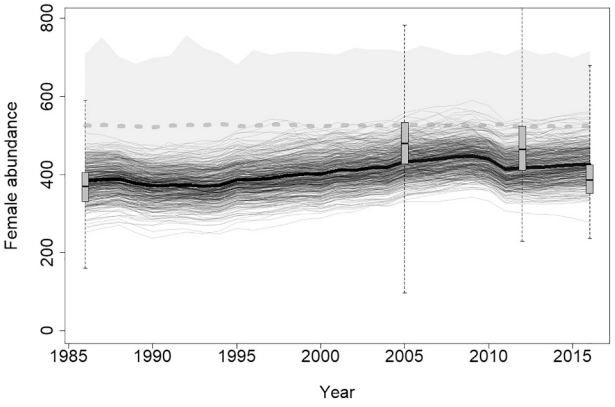

Fig. 3. Scenario 1 population reconstruction: a sample of retrospective projections for female polar bears, 1986–2016, using the theta-logistic equation. The thin black lines are individual stochastic projections. The thick black line is the mean value of projected subpopulation abundance. In the background, the dashed light-gray line is the mean environmental carrying capacity (K) and the light-gray polygon represents the 95% confidence intervals on K. The box plots show the median, first and third quartiles, and range of empirical estimates of female abundance from capture-recapture studies (Obbard et al., 2007) and aerial surveys (Obbard et al., 2015, 2018).

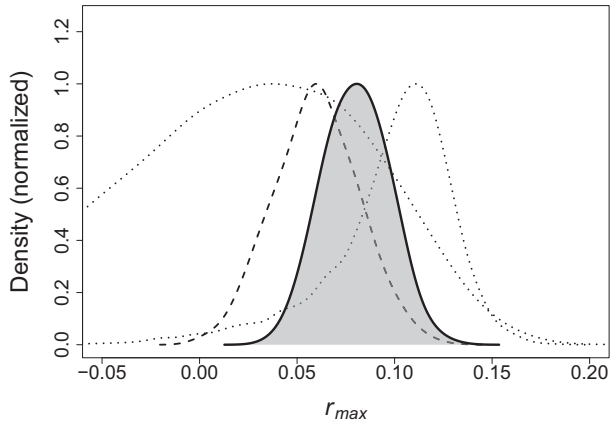

Fig. 4. Distributions of maximum intrinsic growth rate (r_{max}) for the southern Hudson Bay polar bear subpopulation. The solid line with gray shading is the posterior distribution of r_{max} that was estimated using population reconstruction for Scenario 1. The dashed line is the prior for r_{max} derived using estimates of survival and reproduction from other polar bear subpopulations. The two dotted lines are empirical estimates of r_{max} for 1986 (right curve) and 2005 (left curve) based on vital rates estimated from capture-recapture studies.

$P_{t=35}^{N>thresh} = 1.0$) and a negligible probability of extirpation (i.e., $P_{ext} = 0.00$).

For Scenario 3b, the posterior distribution of r_{max} had a mean of 0.08 (95% CI = 0.05–0.11) and the posterior distribution of N/K at the start of population reconstruction had a mean of 0.73 (95% CI = 0.51–0.91). Forward projections started with $\overline{N}_{t=1}/\overline{K}_{t=1} = 0.82$. Although retrospective projections for Scenario 3b resembled those for Scenario 1, K was represented by a logistic function that started to decline rapidly in the mid-2000s. The estimated location of the logistic curve's midpoint was time step $t = 24$ (95% CI = 8–42) of forward projections and the estimated steepness parameter was −0.22 (95% CI = −0.40 to −0.04), corresponding to a projected decline in K of approximately −26% per decade during the period 2016–2049. Although a harvest strategy with $h = 0.01$ corresponded to $P_{t=35}^{N>MNPL} = 0.82$, it also resulted in $P_{ext} = 0.17$ (compared to $P_{ext} = 0.12$ for Scenario 3b with no harvest; Table 1, Fig. 5). Extirpation would be inevitable for a subpopulation experiencing such a rapid and unidirectional decline in K. Furthermore, any

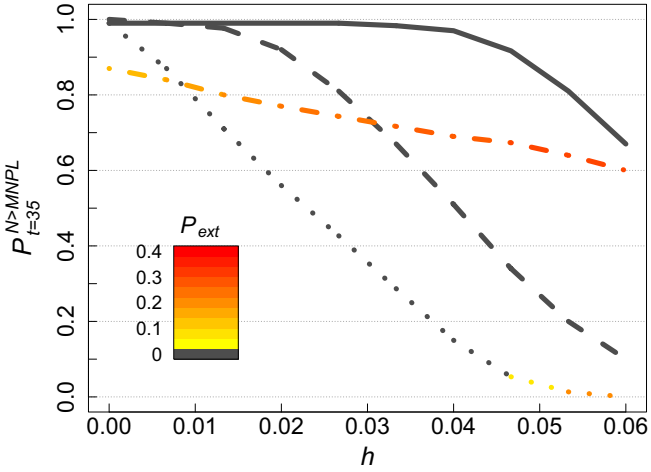

Fig. 5. Probability of meeting Management Objective 1 (maintaining subpopulation abundance [N] above maximum net productivity level [$MNPL$] at time step 35; $P_{t=35}^{N>MNPL}$) as a function of harvest rate (h) for the female segment of the Southern Hudson Bay polar bear subpopulation. Lines correspond to simulations results from Scenario 1 (solid), Scenario 2 (dash), Scenario 3a (dot), and Scenario 3b (dot-dash). Line coloring corresponds to the probability of extirpation (P_{ext}).

reduction in equilibrium subpopulation size due to harvest (i.e., such that $N/K < 1$) would lead to the quasi-extinction threshold being crossed sooner.

4. Discussion

We presented a quantitative harvest risk assessment for the SH polar bear subpopulation that incorporated the potential effects of sea-ice loss, the primary threat to polar bears throughout their range (PBRS, 2015; Atwood et al., 2016; Regehr et al., 2016). We considered alternative scenarios reflecting uncertainty in the subpopulation's status and response to environmental change. Results were a series of harvest strategies and their forecasted demographic outcomes. Our findings should be interpreted with caution given that continued warming could result in complex ecological interactions (e.g., between prey status and habitat availability; Stirling, 2002) and non-linear demographic responses as critical thresholds are passed (Molnár et al., 2020). The risk of accelerating potential climate-related declines in polar bear abundance could be reduced through adherence to a state-dependent management framework and a conservative approach to harvest.

5. Demographic model

Early harvest risk assessments for polar bears used RISKMAN, a stochastic population modeling tool that includes age-specific vital rates and a multiyear reproductive cycle (Taylor et al., 2006b). RISKMAN does not allow for temporal trends in vital rates (e.g., due to habitat loss) or updates to harvest based on periodic population studies. To investigate interactions between habitat loss and human-caused removals, Regehr et al. (2017) proposed a matrix projection model that is based on the polar bear life cycle, includes density dependence, and links management with research. We used a state-dependent management framework like Regehr et al., 2017 but with a simpler demographic model due to sparse data for the SH subpopulation. In contrast with the matrix model, the theta-logistic equation used here did not include sex or age structure, a mechanistic representation of reproduction and maternal care, or positive density dependence (i.e., Allee effects). Although Johnson et al. (2018) found that a theta-logistic population model performed similarly to an age-structured matrix model when evaluating sustainable harvest for taiga bean geese (*Anser fabalis fabalis*),

it is possible that ignoring demographic autocorrelation (e.g., due to dependence between mothers and cubs) led to an underestimate of variance in our projections. The theta-logistic equation also did not include individual differences in reproductive value, harvest vulnerability, or energetic requirements. One ramification was that we could not evaluate sex-selective harvest, a widely applied management tool for polar bears (Taylor et al., 2008). A demographic assessment that considers population composition and selective removals would require up-to-date estimates of vital rates and their relationships with the environment, which can be obtained from studies that identify individual animals (e.g., physical or genetic capture-recapture; Lunn et al., 2016).

The discrete version of the theta-logistic equation allowed nonlinear density dependence in population growth rate, which made it possible to focus on interactions between harvest and habitat loss, the dynamic of primary interest. Management Objective 1 ($P_{t=35}^{N>MNPL}$) was robust to values of the density-dependent parameter θ under a constant-rate harvest. The probabilities of meeting management objectives 2 and 3 ($P_{t=35}^{N>0.9N1}$ and $P_{t=35}^{N>thresh}$, respectively) declined with θ because these objectives were defined relative to static abundance thresholds, and lower values of θ were associated with lower values of *MNPL*, r_{MNPL}, and equilibrium subpopulation size (Supporting File 5). At $\theta = 1$, the theta-logistic equation reduces to the standard logistic model of density dependence with $MNPL = 0.5K$ and $r_{MNPL} = 0.5r_{max}$. If demographic behaviors of the SH subpopulation were characterized by a value of θ close to 1, the subpopulation would be less resilient and support lower harvest levels than indicated by our analyses. We suggest this is unlikely, however, given that population dynamics theory and empirical data for large mammals indicate that most density-dependent changes occur at high relative densities (i.e., as $N/K \rightarrow 1$; Fowler, 1987; Wade, 1998; Sinclair, 2003) and *MNPL* for polar bears has been suggested to occur near 0.70 *K* (Regehr et al. 2017) and between 0.75 and 0.90 *K* (Derocher and Taylor, 1994).

During forward projections to evaluate harvest, we assumed that polar bears could experience both density-dependent and density-independent effects because sea-ice loss has both spatial and temporal components (Stern and Laidre, 2016). Recent harvest risk assessments using matrix models have focused on the effects of a declining *K* (e.g., Regehr et al., In press), which is likely reasonable for subpopulations that are in the early stages of habitat loss and have scientific studies capable of detecting changes in r_{max}. For the SH subpopulation, we considered habitat-driven changes in both *N* and r_{max} because *N* may already be declining, and current research methods (aerial surveys) do not provide information on body condition, vital rates, or other factors that could signal a changing r_{max}. Investigating the mechanisms of population change due to habitat loss and exploring mechanistic links between *K* and r_{max} (e.g., using data for well-studied subpopulations such as WH [Lunn et al., 2016]) remain important areas of research.

6. State-dependent management framework

Our analyses assumed there will be a state-dependent harvest management framework in place for the SH subpopulation that can respond to future changes in subpopulation status. This framework requires a coupled research-management system that can monitor harvest, obtain estimates of abundance every five years with similar precision to recent aerial surveys (Obbard et al., 2015, 2018), and use this information to update harvest levels. Such a management framework for SH bears is likely, based on the subpopulation's research history (Dyck et al., 2019) and the existence of a Southern Hudson Bay Polar Bear Advisory Committee, which was established in 2018 to coordinate management among the responsible governmental and Indigenous organizations. If the conditions of such a framework are not met, lower harvest levels than suggested here would be necessary to mitigate risk.

We evaluated harvest relative to three potential management objectives but focused on Management Objective 1 (maintaining the equilibrium size of a harvested subpopulation above *MNPL*) because it is biologically meaningful and defined relative to a potentially changing *K*. Unlike Management Objective 2, which sought to maintain a historical level of abundance, Management Objective 1 can be used to balance opportunities for use with protecting population viability when the environment is changing (USFWS, 2016). Management Objective 3 conveyed the probability that abundance would decline to the point where negative small-population effects could occur or emergency management measures might be warranted (with the caveat that the lower threshold of 175 females was a placeholder). Threshold harvest rules, under which harvest is curtailed or closed below a pre-specified abundance level, can be an effective conservation measure (Fuller et al., 2015). In the future, our modeling framework could be expanded to evaluate alternative management objectives (e.g., more permissive harvest around communities at certain times of the year, to address public safety concerns) and for cost-benefit analyses regarding how changes to the management interval or precision of population data affect harvest risk.

7. Status of the SH polar bear subpopulation

Assessing long-term trends in the SH subpopulation is complicated by differences in the design and geographic extent of research studies, statistical uncertainty in parameter estimates, incomplete harvest reporting in some jurisdictions, and lack of recent movement data to delineate in situ demographic changes from immigration and emigration. There is evidence of a likely decline in this subpopulation from 943 total bears (i.e., female and male) in 2012 (Obbard et al., 2015) to 780 in 2016 (Obbard et al., 2018) based on aerial surveys with similar methodology. This appears consistent with habitat loss and documented declines in body condition (Obbard et al., 2016). When Hudson Bay is ice free in the summer and autumn, the SH and adjacent WH subpopulations are largely segregated (Peacock et al., 2010; Obbard et al., 2015). The WH subpopulation has experienced long-term declines in body condition (Sciullo et al., 2016) and abundance (Regehr et al., 2007; Lunn et al., 2016). Similar to the SH subpopulation, aerial surveys suggest that WH subpopulation abundance declined between 2011 and 2016 (Stapleton et al., 2014; Dyck et al., 2017). Collectively, these findings suggest that the most recent abundance estimate for the SH subpopulation (Obbard et al., 2018) is the result of broader ecosystem change (Ferguson et al., 2010) rather than emigration of bears to the north and west. In contrast to these interpretations, IK indicates that the SH subpopulation is stable or increasing, with general agreement that the number of bears currently observed by community members is the highest over the last five decades (Tonge and Pulfer, 2011; Laforest et al., 2018; NMRWB, 2018).

Our estimate of $r_{max} = 0.10$ for the 1980s is high compared to a mean unharvested growth rate of 0.05 (95% CI = 0.02–0.09) for 10 polar bear subpopulations reviewed by Regehr et al. (2017). If unbiased, this suggests that the SH subpopulation was capable of strong growth and could support a relatively high harvest in the 1980s. In contrast, $r_{max} = 0.01$ for the 2000s is low. We suspect this estimate is influenced by negative bias in estimated survival probabilities (Obbard et al., 2007), which is common at the end of capture-recapture studies for mobile animals (Devineau et al., 2006). If r_{max} had been this low, the observed female harvest rate of approximately 0.05 would likely have caused large reductions in abundance. Nonetheless, it is possible that harvest was a factor in the apparent decline between 2012 and 2016.

8. Sustainable harvest under climate change

The optimistic Scenario 1 assumed that the status of the SH subpopulation for the next 34 years will be like the past 30 years, that *K* will decline gradually in proportion to projected ice-covered days, that the decline in *N* between 2012 and 2016 either was a statistical anomaly or a transient phenomenon, and that continued ice loss will have only minor

density-dependent effects. A starting harvest level of $\overline{H}_{t=1} = 21$ female bears/year met Management Objective 1 at the placeholder degree of risk tolerance (Table 1). This is close to the mean observed harvest for the period 1986–2016 (Supporting File 1), suggesting that our model reproduced plausible demographic behaviors for the SH subpopulation. Considering evidence for habitat loss (Stern and Laidre, 2016), ecosystem change (Ferguson et al., 2010), and apparent declines in abundance of the SH subpopulation (Obbard et al., 2015, 2018), Scenario 1 likely represents an overly optimistic basis for determining the demographic effects of harvest.

Scenarios 3a and 3b represented pessimistic assumptions with different ramifications. Scenario 3a assumed that the SH subpopulation has experienced, or soon will experience, strong density-independent limitation, and that K and r_{max} will continue to decline. This scenario demonstrates the potential for severe overexploitation when capacity for growth is compromised (Table 1). Scenario 3b assumed that the SH subpopulation would maintain its capacity for growth, provided sufficient habitat, but that K would collapse due to sea-ice loss. Although a relatively high r_{max} allowed for a compensatory response to harvest (e.g., $P_{t=35}^{N>MNPL}$ was insensitive to h compared to Scenario 3a; Table 1), even minor reductions in equilibrium subpopulation size due to harvest increased the probability of crossing the quasi-extinction threshold, thus increasing P_{ext}. Under conditions like Scenario 3b, loss of 26% of K per decade would lead to extirpation within 50 years and the primary effect of harvest would be to hasten this outcome.

We evaluated a wide range of harvest strategies, some of which may not be viable management options. To inform tradeoffs between protection and use, it can be helpful to take a strategy that would be considered sustainable under one environmental scenario and evaluate it under a different scenario (Table 1). For example, $h = 0.060$ was unlikely to have undesired demographic effects under the optimistic Scenario 1. However, under the middle-of-the-road Scenario 2, this harvest rate would lead to a high probability of subpopulation abundance below *MNPL* ($P_{t=35}^{N>MNPL} = 0.10$), a moderate probability of depletion ($P_{t=35}^{N>thresh} = 0.52$), and a non-negligible probability of extirpation ($P_{ext} = 0.06$; Table 1). Under Scenarios 3a and 3b, this harvest rate was associated with even more negative outcomes.

Considering the range of conditions explored, we suggest that Scenario 2 is a reasonable starting point for discussions about the demographic effects of harvest on SH polar bears. Scenario 2 represents a subpopulation with an average capacity for growth that experienced a 9% decline in abundance from 2005 to 2016 (i.e., $\overline{N}_{2005} = 455$ and $\overline{N}_{2016} = 415$ from population reconstruction) due to a combination of harvest and declining K. Over the next 34 years, K and r_{max} were projected to decline in proportion to changes in the annual number of ice-covered days. Scenario 2 was informed by harvest and demographic data for the SH subpopulation since 2005 (Obbard et al., 2007, 2015, 2018). Unlike the more optimistic Scenario 1, it did not represent a stable or increasing subpopulation as indicated by IK (Laforest et al., 2018). Nonetheless, Scenario 2 may be consistent with some aspects of IK, including recognition of climate change and—considering that projected subpopulation declines were relatively gradual—the perception that polar bears can exhibit resilience to sea-ice loss (Tonge and Pulfer, 2011; Laforest et al., 2018; NMRWB, 2018). Under Scenario 2, a moderate degree of risk tolerance with respect to Management Objective 1 corresponded to $h \approx 0.02$–0.03 and $\overline{H}_{t=1} \approx 8$–$12$ female bears/year (Table 1). Assuming the SH subpopulation is 50% female, this would be equivalent to a total (i.e., female and male) harvest rate of approximately 0.02–0.03 at a 1:1 male-to-female ratio in removals and a total harvest rate of approximately 0.03–0.045 at a 2:1 male-to-female ratio. For context, the historical standard harvest rate for polar bears, at a 2:1 male-to-female ratio under stable environmental conditions, has been 0.045 (Taylor et al., 1987).

9. Conclusions

The sustainable harvest of wildlife will be influenced by climate change and the mechanisms through which it affects population dynamics. Using polar bears as an example, we present a harvest risk assessment that considers alternative scenarios for the demographic effects of climate-driven habitat loss. Our findings can be used to inform current management and develop quantitative biological hypotheses against which demographic and environmental data can be evaluated (Houlahan et al., 2017). For example, comparing future abundance estimates to model-based projections could provide support for the assumptions of a particular environmental scenario. Given that the near-term effects of climate change on many wildlife populations are variable and incompletely understood (e.g., Deschamps et al., 2017), stochastic risk assessment and state-dependent harvest management will become increasingly important tools for those seeking to balance population protection with continued opportunities for use.

CRediT authorship contribution statement

Eric Regehr: Conceptualization, Methodology, Software, Formal analysis, Writing – original draft, Visualization; Markus Dyck: Data curation, Writing – review and editing; Samuel Iverson: Conceptualization, Writing – review and editing, Project administration, Funding acquisition; David Lee: Conceptualization, Writing – review and editing; Nicholas Lunn: Conceptualization, Data curation, Writing – review and editing; Joseph Northrup: Conceptualization, Data curation, Writing – review and editing, Visualization; Marie-Claude Richer: Data curation, Writing – review and editing; Guillaume Szor: Conceptualization, Data curation, Writing – review and editing; Michael Runge: Methodology, Formal analysis, Writing – review and editing.

Declaration of competing interest

The authors declare no competing interests.

Acknowledgments

Primary funding for E. Regehr was provided by Environment and Climate Change Canada (Award #GCXE20C066) and the University of Washington. Funding for co-authors was provided by the organizations they are affiliated with. Sea-ice data were provided by H. Stern. We thank M. Obbard for insights on the ecology of this subpopulation. We thank all the hunters from Nunavut, Ontario, and Québec that provided harvest samples. Any use of trade, firm, or product names is for descriptive purposes only and does not imply endorsement by the U.S. Government.

Appendix 1. Behaviors of the theta-logistic equation

Key behaviors of the theta-logistic equation can be demonstrated by growth and yield curves (Figs. A1 and A2, respectively). These curves were generated using $r_{max} = 0.06$, a reasonable value for polar bears (Regehr et al., 2017). At low densities, the observed growth rate is equal to the maximum intrinsic growth rate (r_{max}) because crowding and competition are at a minimum (Fig. A1). The observed growth rate remains high until abundance (N) starts to approach environmental carrying capacity (K), at which point growth declines rapidly until stability is reached at an equilibrium abundance $N = K$. This nonlinear density dependence results in an asymmetric yield curve for which maximum net productivity level (*MNPL*),

and thus maximum sustainable yield (*MSY*), occurs at approximately 0.70*K* (Fig. A2). The corresponding ratio r_{MNPL}/r_{max} is approximately 0.83, suggesting relatively strong compensation for human-caused mortality. These demographic behaviors are broadly consistent with those resulting from a stage-structured matrix population model based on the polar bear life cycle (Regehr et al., 2017). It is important to use a biologically realistic model of density dependence when evaluating the combined effects of habitat change and human-caused removals (Williams, 2013).

We evaluated harvest relative to three management objectives. We focused on Management Objective 1, which sought to maintain the equilibrium size of a harvested subpopulation above *MNPL* (Regehr et al., 2017, 2018). This keeps abundance on the right (i.e., conservative) side of the harvest yield curve (Fig. A2), which protects against overharvest while allowing the possibility for harvest levels to approach *MSY* (USFWS, 2016). Since *MNPL* is defined relative to a potentially changing *K*, Management Objective 1 accommodates environmental variation and therefore may be more useful than objectives with a static reference point (e.g., it does not seek to maintain a historical level of abundance, which may be impossible if habitat is declining, as is the case for all polar bear subpopulations [Stern and Laidre, 2016]).

Appendix 1 Literature cited

Regehr EV, Polasek L, Von Duyke A, Wilder JM, Wilson RR (2018) Harvest Risk Assessment for Polar Bears in the Chukchi Sea: Report to the Commissioners of the U.S.–Russia Polar Bear Agreement, 25 June 2018. http://www.adfg.alaska.gov/static/home/library/pdfs/wildlife/research_pdfs/chukchi_polar_bear_harvest_report_final_25june18.pdf.

Regehr EV, Wilson RR, Rode KD, Runge MC, Stern HL (2017) Harvesting wildlife affected by climate change: a modeling and management approach for polar bears. J Appl Ecol 54:1534–1543.

Stern HL, Laidre KL (2016) Sea–ice indicators of polar bear habitat. The Cryosphere 10:2027–2041.

USFWS (2016) Polar bear (*Ursus maritimus*) conservation management plan, final. US Fish and Wildlife Service, Region 7, Anchorage, Alaska. https://www.fws.gov/alaska/pages/what-we-do/marine-mammals/polar-bear-program/Plan.

Williams CK (2013) Accounting for wildlife life-history strategies when modeling stochastic density-dependent populations: a review. Journal of Wildlife Management 77:4–11.

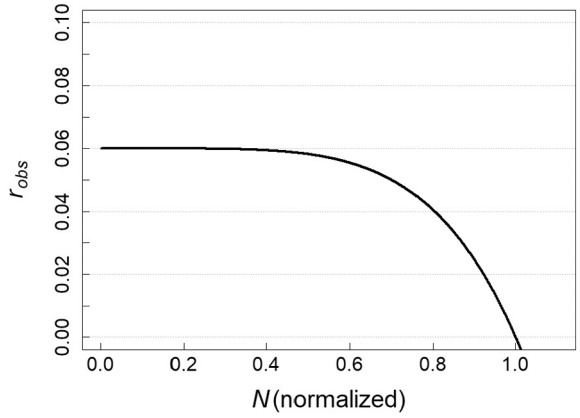

Fig. A1. Example growth curve derived from a theta-logistic equation with the density-dependent shape parameter $\theta = 5.045$ and maximum intrinsic growth rate $r_{max} = 0.06$. The x-axis is normalized abundance (N) such that environmental carrying capacity (K) occurs at $N = 1$. The y-axis is the observed growth rate (r_{obs}), which is equivalent to r_{max} at low densities and declines rapidly to 0 as $N/K \rightarrow 1$.

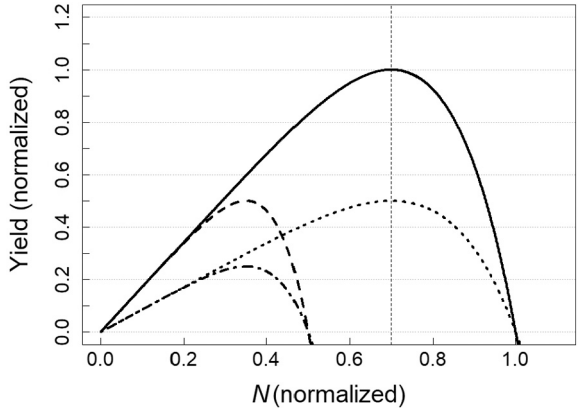

Fig. A2. Example yield curves derived from a theta-logistic equation with the density-dependent shape parameter $\theta = 5.045$. The solid black line is an example baseline curve with environmental carrying capacity $K = 1$ and maximum intrinsic growth rate $r_{max} = 0.06$. The x-axis is normalized abundance (N) such that environmental carrying capacity occurs at $N = 1$ for the baseline curve. The y-axis is normalized yield such that maximum sustainable yield $MSY = 1$ for the baseline curve. The vertical dashed line represents maximum net productivity level (*MNPL*), the subpopulation abundance at which *MSY* is achieved for the baseline curve. The dotted line shows the yield curve if r_{max} was reduced to 0.03. The dashed line shows the yield curve if K was reduced to 0.5. The dot-dash line shows the yield curve if both r_{max} and K were reduced.

Appendix 2. Supplementary data

Supplementary data to this article can be found online at https://doi.org/10.1016/j.biocon.2021.109128.

References

Amstrup, S.C., 2003. Polar bear, *Ursus maritimus*. In: Feldhamer, G.A., Thompson, B.C., Chapman, J.A. (Eds.), Wild Mammals of North America: Biology, Management, and Conservation. The Johns Hopkins University Press, Baltimore, pp. 587–610.

Atwood, T.C., Marcot, B.G., Douglas, D.C., Amstrup, S.C., Rode, K.D., Durner, G.M., Bromaghin, J.F., 2016. Forecasting the relative influence of environmental and anthropogenic stressors on polar bears. Ecosphere 7, e01370.

Bowyer, R.T., Boyce, M.S., Goheen, J.R., Rachlow, J.L., 2019. Conservation of the world's mammals: status, protected areas, community efforts, and hunting. J. Mammal. 100, 923–941.

Derocher, A.E., Taylor, M., 1994. Density-dependent population regulation of polar bears. Int. Conf. Bear Res. Manag. Monogr. 3, 25–37.

Descamps, S., Aars, J., Fuglei, E., Kovacs, K.M., Lydersen, C., Pavlova, O., Pedersen, A.O., Ravolainen, V., Strom, H., 2017. Climate change impacts on wildlife in a High Arctic archipelago - Svalbard, Norway. Glob. Chang. Biol. 23, 490–502.

Devineau, O., Choquet, R., Lebreton, J.D., 2006. Planning capture–recapture studies: straightforward precision, bias, and power calculations. Wildl. Soc. Bull. 34, 1028–1035.

Durner, G.M., Laidre, K.L., York, G.S. (Eds). 2018. Polar Bears: Proceedings of the 18th Working Meeting of the IUCN/SSC Polar Bear Specialist Group, 7–11 June 2016, Anchorage, Alaska. IUCN, Gland, Switzerland and Cambridge, UK.

Dyck, M., Campbell, M., Lee, D., Boulanger, J., Hedman, D., 2017. 2016 Aerial Survey of the Western Hudson Bay Polar Bear Subpopulation. Final Report. Government of Nunavut, Department of Environment, Wildlife Research Section, Igloolik, Nunavut. Available at: https://gov.nu.ca/sites/default/files/pb_wh_2016_population_assessment_gn_report_27_june_2017.pdf.

Dyck, M., Gilbert, G., Iverson, S., Lunn, N.J., Northrup, J.M., Penn, A., Richer, M.-C., Szor, G., 2019. Re-assessment of the southern Hudson Bay polar bear subpopulation. Report to Southern Hudson Bay Polar Bear Subpopulation Advisory Committee From the Southern Hudson Bay Polar Bear Technical Working Group, 11 September 2019. Unpublished report, 39 pp.

Ferguson, S.H., Loseto, L.L., Mallory, M.L. (Eds.), 2010. A Little Less Arctic: Top Predators in the World's Largest Northern Inland Sea. Springer, New York.

Fowler, C.W., 1987. A review of density dependence in populations of large mammals. Curr. Mammal. 1, 401–441.

Fuller, E., Brush, E., Pinsky, M.L., 2015. The persistence of populations facing climate shifts and harvest. Ecosphere 6, 153.

Houlahan, J.E., McKinney, S.T., Anderson, T.M., McGill, B.J., 2017. The priority of prediction in ecological understanding. Oikos 126, 1–7.

Hunter, C.M., Caswell, H., Runge, M.C., Amstrup, S.C., Regehr, E.V., Stirling, I., 2007. Polar Bears in the Southern Beaufort Sea II: Demography and Population Growth in Relation to Sea Ice Conditions. USGS Alaska Science Center, Anchorage, Administrative Report 46 pp.

Hunter, C.M., Caswell, H., Runge, M.C., Amstrup, S.C., Regehr, E.V., Stirling, I., 2010. Climate change threatens polar bear populations: a stochastic demographic analysis. Ecology 91, 2883–2897.

IPCC – Intergovernmental Panel on Climate Change, 2019. Technical summary [Pörtner, H.-O., Roberts, D.C., Masson-Delmotte,V., Zhai, P., Poloczanska, E., Mintenbeck, K., Tignor, M., Alegría, A., Nicolai, M., Okem, A., Petzold, J., Rama, B., Weyer, N.M. (Eds.)]. In: Pörtner, H.-O., Roberts, D.C., Masson-Delmotte, V., Zhai, P., Tignor, M., Poloczanska, E., Mintenbeck, K., Alegría, A., Nicolai, M., Okem, A., Petzold, J., Rama, B., Weyer, N.M. (Eds.), IPCC Special Report on the Ocean and Cryosphere in a Changing Climate. https://www.ipcc.ch/srocc/chapter/technical-summary/.

Johnson, F.A., Alhainen, M., Fox, A.D., Madsen, J., Guillemain, M., 2018. Making do with less: must sparse data preclude informed harvest strategies for European waterbirds? Ecol. Appl. 28, 427–441.

Kolenosky, G.B., Abraham, K.F., Greenwood, C.J., 1992. Polar Bears of Southern Hudson Bay. Polar Bear Project, 1984–88. Final Report. Ontario Ministry of Natural Resources, Maple, Ontario, Canada (107 pp).

Kolenosky, G.B., Pond, B.A., Abraham, K.F., 1994. Population characteristics of polar bears in Southern Hudson Bay (abstract only). Int. Conf. Bear Res. Manag. 9, 301.

Laforest, B.J., Hébert, J.S., Obbard, M.E., Thiemann, G.W., 2018. Traditional ecological knowledge of polar bears in the northern Eeyou Marine Region, Québec, Canada. Arctic 71, 40–58.

Laidre, K.L., Stern, H., Kovacs, K.M., Lowry, L., Moore, S.E., Regehr, E.V., Ferguson, S.H., Wiig, Ø., Boveng, P., Angliss, R.P., Born, E.W., Litovka, D., Quakenbush, L., Lydersen, C., Vongraven, D., Ugarte, F., 2015. Arctic marine mammal population status, sea ice habitat loss, and conservation recommendations for the 21st century. Conserv. Biol. 29, 724–737.

Lunn, N.J., Servanty, S., Regehr, E.V., Converse, S.J., Richardson, E., Stirling, I., 2016. Demography of an apex predator at the edge of its range: impacts of changing sea ice on polar bears in Hudson Bay. Ecol. Appl. 26, 1302–1320.

Molnár, P.K., Bitz, C.M., Holland, M.M., Kay, J.E., Penk, S.R., Amstrup, S.C., 2020. Fasting season length sets temporal limits for global polar bear persistence. Nat. Clim. Chang. 10, 732.

Nilsen, E.B., Strand, O., 2018. Integrating data from multiple sources for insights into demographic processes: simulation studies and proof of concept for hierarchical change-in-ratio models. PLoS One 13, e0194566.

NMRWB – Nunavik Marine Region Wildlife Board, 2018. Nunavik Inuit knowledge and observations of polar bears: polar bears of the Southern Hudson Bay subpopulation. Project conducted and report prepared for the NMRWB by Basterfield, M., Breton–Honeyman, K., Furgal, C., Rae, J., O'Connor, M. Available at: https://nmrwb.ca/wp-content/uploads/2017/05/NMRWB-Nunavik-Inuit-knowledge-and-Observations-of-polar-bears-SHB-subpopulation.pdf.

Obbard, M.E., McDonald, T.L., Howe, E.J., Regehr, E.V., Richardson, E.S., 2007. Polar Bear Population Status in Southern Hudson Bay, Canada. U.S. Geological Survey Administrative Report, Reston, Virginia.

Obbard, M.E., Thiemann, G.W., Peacock, E., DeBruyn, T.D. (Eds.), 2010. Polar Bears: Proceedings of the 15th Working Meeting of the IUCN/SSC Polar Bear Specialist Group, 29 June – 3 July 2009, Copenhagen, Denmark. IUCN, Gland, Switzerland and Cambridge, UK.

Obbard, M.E., Stapleton, S., Middel, K.R., Thibault, I., Brodeur, V., Jutras, C., 2015. Estimating the abundance of the Southern Hudson Bay polar bear subpopulation with aerial surveys. Polar Biol. 38, 1713–1725.

Obbard, M.E., Cattet, M.R.L., Howe, E.J., Middel, K.R., Newton, E.J., Kolenosky, G.B., Abraham, K.F., Greenwood, C.J., 2016. Trends in body condition in polar bears (*Ursus maritimus*) from the Southern Hudson Bay subpopulation in relation to changes in sea ice. Arctic Sci. 2, 15–32.

Obbard, M.E., Stapleton, S., Szor, G., Middel, K.R., Jutras, C., Dyck, M., 2018. Re–assessing abundance of Southern Hudson Bay polar bears by aerial survey: effects of climate change at the southern edge of the range. Arctic Sci. 4, 634–655.

PBRS – Polar Bear Range States, 2015. Circumpolar action plan: conservation strategy for polar bears. A product of the representatives of the parties to the 1973 agreement on the conservation of polar bears. http://polarbearagreement.org/circumpolar-action-plan.

Peacock, E., Derocher, A.E., Lunn, N.J., Obbard, M.E., 2010. Polar bear ecology and management in Hudson Bay in the face of climate change. In: Ferguson, S.H., Loseto, L.L., Mallory, M.L. (Eds.), A Little Less Arctic: Top Predators in the World's Largest Northern Inland Sea. Springer, New York, pp. 93–115.

Post, E., Alley, R.B., Christensen, T.R., Macias-Fauria, M., Forbes, B.C., Gooseff, M.N., Iler, A., Kerby, J.T., Laidre, K.L., Mann, M.E., Olofsson, J., Stroeve, J.C., Ulmer, F., Virginia, R.A., Wang, M., 2019. The polar regions in a 2°C warmer world. Sci. Adv. 5, eaaw9883.

Regehr, E.V., Lunn, N.J., Amstrup, S.C., Stirling, I., 2007. Effects of earlier sea ice breakup on survival and population size of polar bears in western Hudson Bay. J. Wildl. Manag. 71, 2673–2683.

Regehr, E.V., Laidre, K.L., Akçakaya, H.R., Amstrup, S.C., Atwood, T.C., Lunn, N.J., Obbard, M., Stern, H., Thiemann, G.W., Wiig, Ø., 2016. Conservation status of polar bears (*Ursus maritimus*) in relation to projected sea–ice declines. Biol. Lett. 12, 20160556 https://doi.org/10.1098/rsbl.2016.0556.

Regehr, E.V., Runge, M.C., Von Duyke, A., Wilson, R.R., Polasek, L., Rode, K.D., Hostetter, N.J., Converse, S.J., 2021. Demographic risk assessment for a harvested species threatened by climate change: polar bears in the Chukchi Sea. Ecol. Appl. In press.

Regehr, E.V., Wilson, R.R., Rode, K.D., Runge, M.C., Stern, H.L., 2017. Harvesting wildlife affected by climate change: a modeling and management approach for polar bears. J. Appl. Ecol. 54, 1534–1543.

Runge, M.C., Sauer, J.R., Avery, M.L., Blackwell, B.F., Koneff, M.D., 2009. Assessing allowable take of migratory birds. J. Wildl. Manag. 73, 556–565.

Sciullo, L., Thiemann, G.W., Lunn, N.J., 2016. Comparative assessment of metrics for monitoring the body condition of polar bears in Western Hudson Bay. J. Zool. 300, 45–58.

Sinclair, A.R.E., 2003. Mammal population regulation, keystone processes and ecosystem dynamics. Philos. Trans. R. Soc. B 358, 1729–1740.

Stapleton, S., Atkinson, S., Hedman, D., Garshelis, D., 2014. Revisiting Western Hudson Bay: using aerial surveys to update polar bear abundance in a sentinel population. Biol. Conserv. 170, 38–47.

Stern, H.L., Laidre, K.L., 2016. Sea–ice indicators of polar bear habitat. Cryosphere 10, 2027–2041.

Stirling, I., 2002. Polar bears and seals in the eastern Beaufort Sea and Amundsen Gulf: a synthesis of population trends and ecological relationships over three decades. Arctic 55, 59–76.

Stubben, C., Milligan, B., 2007. Estimating and analyzing demographic models using the popbio package in R. J. Stat. Softw. 22, 1–23.

Taylor, M.K., DeMaster, D.P., Bunnell, F.L., Schweinsburg, R.E., 1987. Modeling the sustainable harvest of female polar bears. J. Wildl. Manag. 51, 811–820.

Taylor, M.K., Laake, J., McLoughlin, P.D., Cluff, H.D., Messier, F., 2006a. Demographic parameters and harvest–explicit population viability analysis for polar bears in M'Clintock Channel, Nunavut, Canada. J. Wildl. Manag. 70, 1667–1673.

Taylor, M., Obbard, M., Pond, B., Kuc, M., Abraham, D., 2006b. A Guide to Using RISKMAN: Stochastic and Deterministic Population Modeling RISK MANagement Decision Tool for Harvested and Unharvested Populations. The Queen's Printer for Ontario, Ontario, Canada. Available at. http://riskman.nrdpfc.ca/downloads/RiskmanManual.pdf.

Taylor, M.K., McLoughlin, P.D., Messier, F., 2008. Sex-selective harvesting of polar bears *Ursus maritimus*. Wildl. Biol. 14, 52–60.

Tonge, M.B., Pulfer, T.L., 2011. Recovery strategy for polar bear (Ursus maritimus) in Ontario. Ontario recovery strategy series. Prepared for the Ontario Ministry of Natural Resources, Peterborough, Ontario. Available at. https://files.ontario.ca/environment-and-energy/species-at-risk/stdprod_086036.pdf.

USFWS – United States Fish and Wildlife Service, 2016. Polar Bear (*Ursus maritimus*) Conservation Management Plan, Final. US Fish and Wildlife Service, Region 7, Anchorage, Alaska. Available at. https://www.fws.gov/alaska/pages/what-we-do/marine-mammals/polar-bear-program/Plan.

Wade, P.R., 1998. Calculating limits to the allowable human–caused mortality of cetaceans and pinnipeds. Mar. Mammal Sci. 14, 1–37.